



Università degli Studi di Cagliari

Facoltà di Scienze Matematiche, Fisiche e Naturali

Laurea Magistrale in Fisica

# Observation-guided Simulation of the Extragalactic Binary Gravitational Wave Foreground

Relatore:

**Prof. Riccardo Murgia**

Co-relatori:

**Prof. Thomas Kupfer**

**Weitian Yu**

Candidato:

**Gabriele Todde**



# Contents

<b>1</b>	<b>Theoretical Framework</b>	<b>7</b>
1.1	Gravitational waves theory . . . . .	7
1.1.1	Gravitational Waves as Perturbations . . . . .	7
1.1.2	Motion and geodesics . . . . .	9
1.1.3	The Quadrupole Approximation . . . . .	9
1.1.4	Gravitational waves from a binary system . . . . .	9
1.1.5	Energy carried by a gravitational wave . . . . .	9
1.1.6	Evolution of a compact binary system . . . . .	9
1.2	White dwarfs and galaxies . . . . .	9
1.2.1	White dwarfs . . . . .	9
1.2.2	Galaxies . . . . .	9
1.3	LISA . . . . .	10
1.4	interferometers . . . . .	10
<b>2</b>	<b>Methods and Data</b>	<b>11</b>
2.1	Stellar populations synthesis codes . . . . .	11
2.1.1	The starting point . . . . .	12
2.1.2	Single star evolution . . . . .	13
2.1.3	Binary stars evolution . . . . .	13
2.2	COSMIC . . . . .	14
2.2.1	Fixed population . . . . .	14
2.2.2	Astrophysical population . . . . .	16
2.3	GWGC and Galaxy Properties . . . . .	17
2.3.1	What it has vs what we need . . . . .	17
2.3.2	Mass-luminosity relation . . . . .	18
2.3.3	Mass-metallicity relation . . . . .	19
2.3.4	Missing galaxies . . . . .	20
2.4	Final considerations . . . . .	22
2.4.1	The final fixed populations . . . . .	23
2.4.2	LISA's frequency resolution . . . . .	24
<b>3</b>	<b>Results</b>	<b>25</b>
<b>4</b>	<b>Conclusions and Future Perspectives</b>	<b>27</b>

CONTENTS	4
----------	---

---

A Appendix	29
------------	----

# Introduction

In the context of the gravitational waves study, there are mainly two possible paths: the first is the **analysis of existing data** from experiments like Ligo, Virgo and Kagra, with the goal of detecting and characterizing the observable sources within their relative frequency bands; the second approach is the **forecasting approach**, which aims to characterize future experiments in order to better understand what types of sources they could detect and how well.

One of the most important future detectors is the European *Laser Interferometer Space Antenna* (LISA), the first space-based gravitational wave detector. LISA will be arranged as an equilateral triangle with 2.5 million kilometers long arms, placed in a heliocentric orbit, and will operate within the frequency range from approximately 0.1mHz to 1Hz. Among the typical sources that emit gravitational wave signal in this range are the **compact binaries**, and in our particular case we are interested in **double white dwarf binaries** (WDBs).

The goal of this work is to estimate the gravitational wave background produced by the extragalactic WDBs in the local universe, by using the **COSMIC** code to generate synthetic astrophysical populations to represent the galaxies listed in the **Gravitational Wave Galaxy Catalog** (GWGC).

In **Chapter 1** we will introduce the theoretical foundations of gravitational waves, derive the amplitude of the signal generated by a binary system, and define the most important parameters. Finally, we discuss how to combine the signals from multiple sources, to find a cumulative background.

In **Chapter 2** we will give a brief overview of how gravitational wave detectors work, trying to better understand what kinds of sources LISA will be able to see, what resolution and what sensitivity it will have and why in particular we are interested in WDBs.

In **Chapter 3** we introduce the concept of stellar population synthesis and the code COSMIC used for this purpose. We will introduce its features, main parameters, and pipeline, and explain how it is used to generate full-size astrophysical populations of WDBs.

In **Chapter 4** we introduce the GWGC, list the key information it provides and explain how we move from there to infer the remaining parameters that we need.

In **Chapter 5** we use the obtained information to compute the total gravitational wave signal summing the contribution from all the simulated sources, taking into account their spatial distribution, LISA's frequency resolution, and the *zone of avoidance* caused by the milky way.

In **Chapter 6** we plot the total resulting signal on the LISA sensitivity curve, and discuss the results and their possible implications.

Finally, in **Chapter 7** we will draw some conclusions from the work as a whole, discussing its limitations, assumptions and its possible extensions and follow-ups.

# Chapter 1

## Theoretical Framework

### 1.1 Gravitational waves theory

After considering, in 1905, the problem of the apparently *instantaneous* propagation of light, with the theory of Special Relativity, in 1916 Albert Einstein considered the problem of the apparently *instantaneous* propagation of gravity through *long distances*, in his theory of General Relativity. Einstein showed that long-distance interaction arises from the deformation of space time caused by massive objects. Hence, in the "static case", the deviated motion apparently caused by the interaction between two distant masses really is, in fact, a manifestation of space time curvature nearby, generated by the presence of the two objects. The "static case" just depicted, though, treats the curvature as if it had always been there, and doesn't take into account of any variation in the masses, positions or velocities of the two objects, that would induce an evolution to the curvature itself. In truth, after a change in the mass-energy distribution, the corresponding curvature variation requires its time to reach far distances, and a fascinating prediction of General Relativity is that it propagates in the form of a wave, that travels at the speed of light.

#### 1.1.1 Gravitational Waves as Perturbations

The typical approach to the study of gravitational waves is to derive them as small perturbations of the background from the Einstein's equations:

$$G_{\mu\nu} = R_{\mu\nu} - \frac{1}{2}g_{\mu\nu}R, \quad (1.1)$$

which can be conveniently written as

$$R_{\mu\nu} = \frac{8\pi G}{c^4} \left( T_{\mu\nu} - \frac{1}{2}g_{\mu\nu}T \right), \quad (1.2)$$

where  $G_{\mu\nu}$  is the Einstein tensor,  $R_{\mu\nu}$  is the Ricci tensor,  $R$  is the Ricci scalar,  $g_{\mu\nu}$  is the metric of space time, and  $T_{\mu\nu}$  is the stress-energy tensor. As a background solution we can consider the flat space time described by the metric  $\eta_{\mu\nu}$ , to which

the perturbation term appears as a fluctuation in the metric  $|h_{\mu\nu}| \ll |\eta_{\mu\nu}|$ , known as *weak field* approximation. Thus, the perturbed space time can be written as:

$$g_{\mu\nu} = \eta_{\mu\nu} + h_{\mu\nu}, \quad |h_{\mu\nu}| \ll |\eta_{\mu\nu}|.$$

With this metric, the equations 1.2 becomes

$$\{\square_F h_{\mu\nu} - \left[ \frac{\partial^2}{\partial x^\lambda \partial x^\mu} h_\nu^\lambda + \frac{\partial^2}{\partial x^\lambda \partial x^\nu} h_\mu^\lambda + \frac{\partial^2}{\partial x^\nu \partial x^\mu} h_\lambda^\lambda \right]\} = -\frac{16\pi G}{c^4} \left( T_{\mu\nu} - \frac{1}{2} \eta_{\mu\nu} T \right).$$

Now, by requiring that the *weak-field* approximation remains satisfied for infinitesimal diffeomorphisms, and by choosing a coordynate system in which the *harmonic gauge condition*<sup>1</sup> is satisfied, we can find that, up to first order in  $h_{\mu\nu}$ , the harmonic gauge condition is equivalent to

$$\frac{\partial}{\partial x^\mu} h_\rho^\mu = \frac{1}{2} \frac{\partial}{\partial x^\rho} h, \quad h = \eta^{\mu\nu} h_{\mu\nu} \equiv h_\nu^\nu, \quad (1.3)$$

and after defining the tensor<sup>2</sup>

$$\bar{h}_{\mu\nu} \equiv h_{\nu\mu} - \frac{1}{2} \eta_{\mu\nu} h,$$

we can finally write the linearized Einstein equations as

$$\begin{cases} \square \bar{h}_{\mu\nu} = -\frac{16\pi G}{c^4} T_{\mu\nu}, \\ \partial^\mu \bar{h}_{\mu\nu} = 0. \end{cases}$$

This form, and its twin with  $T_{\mu\nu} = 0$ , where the first equation becomes the D'Alembert equation, are relevant because they show that *a perturbation of a flat space time propagates as a wave travelling at the speed of light*.

<sup>1</sup>It is an arbitrary coordinate condition which makes it possible to solve the Einstein field equations. It can be found by requiring that the linearized Einstein equations satisfy the D'Alembert equation.

<sup>2</sup>Also known as *trace-reversed* perturbation tensor, since  $\bar{h} = \eta^{\mu\nu} \bar{h}_{\mu\nu} = -h$ .



Harmonic gauge

The TT gauge

### 1.1.2 Motion and geodesics

The motion deviation

The geodesic deviation

### 1.1.3 The Quadrupole Approximation

The weak-field, slow-motion approximation

The quadrupole formula

Transform to the TT gauge

### 1.1.4 Gravitational waves from a binary system

General solution for circular orbits

Up to 13.86/7 at page 255 of the book.

### 1.1.5 Energy carried by a gravitational wave

Stress-energy pseudo-tensor

Gravitational wave luminosity

### 1.1.6 Evolution of a compact binary system

Signal from inspiralling compact objects

Here we get to the actual amplitude we used, and the parameters involved.

## 1.2 White dwarfs and galaxies

### 1.2.1 White dwarfs

### 1.2.2 Galaxies

Morphological types

Here I introduce Hubble types, explaining general physical differences between them. Later I will introduce the T value notation and how to translate in the Hubble sequence types.

## 1.3 LISA

## 1.4 interferometers

- Instrument description (what is an interferometer, why in space, how it will be made, orbit) - frequency band - what will it see? - frequency resolution - sensibility curve and ASD meaning - Why WD choice in particular?

# Chapter 2

## Methods and Data

The abundance of information of the electromagnetic spectrum allowed us to build highly detailed models of various celestial objects such as stars, both on their individual internal structure and on how this is influenced by the interaction with other bodies, for instance in binary systems. In the pursuit of reaching a greater sensitivity in the gravitational counterpart too, which could potentially reveal new information, or place better constraints on the existing models, these stellar models, when combined with a good theory of gravity, can be used to construct synthetic populations that reproduce observable features like luminosity, color, and chemical composition, which could enable us to predict what their gravitational signal would look like. In gravitational waves research, our observational capabilities are still very limited, and the signals are still comparatively very weak relative to their electromagnetic counterpart. Therefore, methods that rely on simulations can be very useful both to explore how different sources could look like in the gravitational wave domain, and how effectively they could be detected with current or future instruments.

### 2.1 Stellar populations synthesis codes

Generating a synthetic population of stars is a very complex task, that involves multiple steps, each involving important choices. *First*, we need to choose a starting point: we could start from the very beginning of stars formation and simulate all the process from the birth onward, or we could select a later phase in the stars evolution, shared from the most, in order to reduce unnecessary computational power and time consumption. If we want to simulate entire stellar populations choosing a starting point also implies selecting appropriate distributions for the main parameters that characterize the "starting point population", like masses, metallicities, but also orbital parameters for the stars that are in binary systems, like orbital period, distance, and eccentricity. *Second*, we must choose how the stars will evolve from the starting point, and this involves the single star evolution but also the effects that interaction with other stars in binary systems have on it. *Finally*,

we have to decide when we want to stop the simulation, choosing an endpoint that aligns with the needs of this study.

### 2.1.1 The starting point

As we know, in the Hertzsprung-Russel diagram, which plots the *luminosity* of the stars vs their *color index*, most of the stars appear distributed in the **main sequence (MS)**, a continuous and distinctive band. A star's position on this band is determined by its initial mass, and a good rule of thumb is that the most massive stars are hotter, more luminous, and evolve more quickly, while the lower-mass stars burn their fuel more slowly, and remain on the MS longer.

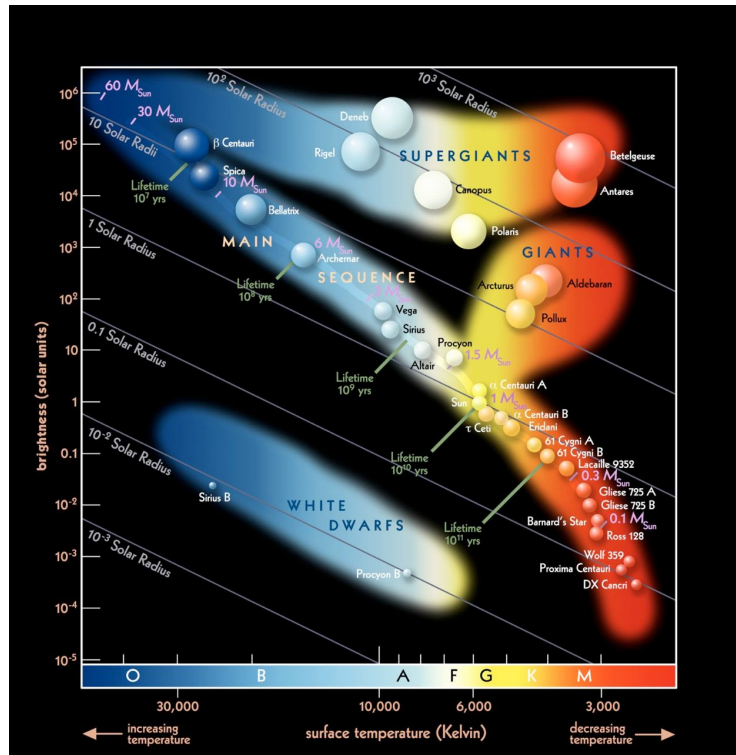


Figure 2.1: WRITE CAPTION, INSERT REFERENCE

Since almost all stars go through a phase in the MS, and evolve from there differently, in this work, the chosen starting point for stellar evolution is the Zero Age Main Sequence (ZAMS). At this stage, stars have just begun hydrogen burning in their cores, marking the start of their stable main sequence phase. This allows to bypass the early phases of star formation, which are much less relevant to the gravitational wave sources of interest, while still capturing the essential evolutionary processes that lead to the formation of compact objects.

### 2.1.2 Single star evolution

Simulating the evolution of a single star is in itself a very complex matter, and the only way to make it computationally feasible in the context of large-scale population synthesis is to approximate the evolution for a wide range of mass  $M$  and metallicity  $Z$ . In fact, detailed evolution codes can require substantial computational time even for the evolution of a single star, which is not practical when generating a full-scale astrophysical population containing millions of stars. Also, in order to make population synthesis statistically robust a large enough number of stars of a certain type must be evolved in order to overcome stochastic noise (in particular, the Poisson noise for  $n$  simulations of a particular type of star, implies an error that grows as  $\sqrt{n}$ ). A winning strategy, adopted by several population synthesis frameworks, is to pre-generate a large grid of detailed stellar evolution models, and use them to derive a number of interpolation formulae as functions that approximate stellar properties as a function of age, mass and metallicity. In Hurley et al. [2000] this method is implemented through the development of a set of **Single Star Evolution (SSE)** formulae, with the result of a very compact, efficient and adaptable code, which makes it perfect for the integration of binary-star interactions. The work presented in Hurley et al. [2000] therefore serves as the theoretical and computational foundation for many complex stellar population synthesis codes, including the one used in this thesis. It takes care of the single-star evolution of stars from ZAMS through all the possible evolutionary outcomes, depending on the star's initial conditions.

### 2.1.3 Binary stars evolution

While the evolution of single stars already represents a challenge, the inclusion of binary interactions introduces a much higher level of complexity. In such systems, the evolution of each star is strongly influenced by its companion through a variety of processes, such as mass transfer and accretion, common envelope evolution, collisions, supernova kicks, tidal effects, angular momentum loss, and mergers. These interactions can drastically alter the final outcomes, and are essential for modeling the formation of compact binaries that are potential gravitational wave targets for LISA. To efficiently model binary evolution within the framework of stellar population synthesis, the work of Hurley et al. [2002] extends the SSE formalism by introducing a set of prescriptions for binary interactions, and updating the treatment of processes such as Roche lobe overflow, common envelope evolution and coalescence by collision, leading to the development of the **Binary Star Evolution (BSE)** algorithm. This code includes the interpolation-based approach used in SSE for single-star evolution, but adds a comprehensive treatment of binary-specific processes, enabling the simulation of a wide range of binary configurations but keeping the affordable computational requirements of SSE. The BSE algorithm tracks the joint evolution of both stars in a binary system, taking into account their initial parameters, such as masses, orbital period, eccentricity, and metallicity, and updates these properties dynamically as the system evolves. The flexibility and speed of the

BSE code make it a key component in many modern population synthesis tools, including the one used in this thesis, which we will now introduce.

## 2.2 COSMIC

For the purposes of this work, we employ a community-developed binary population synthesis (BPS) python-based code, called the **Compact Object Synthesis and Monte Carlo Investigation Code (COSMIC)**, whose «*primary purpose is to generate synthetic populations with an adaptive size based on how the shape of binary parameter distributions change as the number of simulated binaries increases*»<sup>1</sup>. COSMIC's binary evolution is built upon BSE, incorporating extensive modifications in order to include updated physical prescriptions. It includes all necessary tools to generate a population, from the generation of initial conditions, to scaling the simulated systems to full-scale astrophysical populations. The code is presented in Breivik et al. [2020], where it is described in full detail and used, as a proof of concept, to simulate the Galactic population of compact binaries and their associated gravitational wave signal. In the following section we will see the main features of the code, and explain what makes it the right choice for this thesis work.

### 2.2.1 Fixed population

A fundamental concept in COSMIC, which is the key to the code's efficiency, is the idea of *fixed population*. This refers to a relatively small sample<sup>2</sup> of just enough binaries to capture, in a statistically meaningful way, the underlying shape of the parameter distribution functions of the target population, as determined by the user specified Star Formation History (SFH) and evolution model. This is achieved following an iterative process designed to reach a convergence with respect to a defined matching condition, and consists of five key steps:

1. The user selects a binary evolution model and SFH;
2. Based on the SFH and the chosen initial parameter distribution, an initial population is generated;
3. The population evolves for a user specified number of steps, according to the selected evolution model;
4. If it is the first iteration, half of the simulated systems is compared with the total population. In the following steps, the population from the previous one gets compared to the population containing both the current and previous

---

<sup>1</sup><https://cosmic-popsynth.github.io/docs/stable/pages/about.html>

<sup>2</sup>Note that, from now on, every time we talk about sampling, that is where the "M" of COSMIC comes into play: this code uses proficiently the Monte Carlo Markov Chain methods to sample populations and parameter distributions, as will follow in this section.

iterations. In any case, the comparison is done in order to check if the matching condition has been achieved;

5. Once the parameter distributions of the population have converged, the corresponding population is called *fixed population*, which represents the statistical features of a binary evolution model.

In practice, the fixed population is the converged, computationally efficient representation of the systems that we want to simulate, embedded in a complete small-scale synthetic galaxy that also contains other stellar components. The output is stored in a data frame, which separates the full galaxy properties from the fixed population ones. The last step required to construct a full size galaxy is to scale the fixed population (by mass or by number of stars) with a re-sampling approach with replacement, allowing to extrapolate a larger final population that preserves the statistical properties encoded in the fixed population.

### Initialization

The fixed population is generated from an initial collection of binaries sampled from distribution functions to assign to each binary an initial value of metallicity ( $Z$ ), primary star mass ( $m$ ), mass ratio ( $q$ ), orbital separation ( $a$ ), eccentricity ( $e$ ), and birth time ( $T_0$ ) according to the selected SFH. In COSMIC the user can choose between different binary parameter distributions, and different parameters can be treated independently. Moreover, COSMIC allows a complete personalization of the initial population through a number of other parameters, including different time-steps to control the binary physics, metallicity, stellar winds, common envelope phase, natal kicks, remnant mass, remnant spin, gravitational wave orbital decay, mass transfer, tides, and particular specifications for different kinds of stellar objects, mixing variables, and magnetic braking. In this work all the parameters were left default, but one: we tweaked the metallicity value, in order to differentiate fixed populations describing the parameter distributions for galaxies of different types. We will go more into detail on this topic in the next chapters.

### Convergence

The number of simulated systems in the fixed population ideally describes the final parameter distribution functions while being low enough to keep the code efficient. Since every population depends on a different binary evolution model, to quantify this number a *discrete match criteria* is developed, based on the work Chatziioannou et al. [2017]. Independently generated histograms for each parameter are used to track their distribution as successive populations are generated and cumulatively added to the fixed population. The physical limits of the simulated systems are

then enforced by taking the logistic transform, and finally the match is defined as:

$$match = \frac{\sum_{k=1}^N P_{k,i} P_{k,i+1}}{\sqrt{\sum_{k=1}^N (P_{k,i} P_{k,i}) \sum_{k=1}^N (P_{k,i} P_{k,i+1})}}, u$$

where  $P_{k,i}$  is the probability for the  $k$ th bin, for the  $i$ th iteration. For how it is defined, the match value shifts between 0 and 1, and tends to unity as the parameter distributions converge to a distinct shape.

### The output

Since COSMIC uses BSE as its core binary evolution algorithm, the output of COSMIC follows most of the same conventions as BSE. The *kstar values* (e.g. the number that represent a specific stellar type) and evolution stages are nearly identical to their BSE counterparts, and the exact references can be found in the **Appendix**. In order to generate a fixed population, the COSMIC can be ran through a one-line command directly on the terminal, specifying a parameter file, the *kstar values* for the primary and secondary star, the maximum number of systems to evolve, every how many systems to check in, in order to track the distributions of the parameters, and how many processors to use. The final output is in an *hdf5* file containing several data frames, that keep track of various important quantities during the evolution: the total number of stars and total mass of the entire population, the number of binaries, the convergence, and so on. The *conv* data frame contains all the information about the final fixed population, and thus is the one that we will use the most: from it we can extract all the parameter distributions of the fixed population, such as the orbital parameters, and the individual star information. The parameter distributions of a fixed population of binary white dwarfs with a default metallicity value set at 0.020 is shown in **Figure 2.2**.

### 2.2.2 Astrophysical population

Once the convergence criteria is achieved, an astrophysical population can be sampled. The number of sources in the astrophysical population  $N_{astro,tot}$  can be found by upscaling the size of the fixed population,  $N_{fixed}$ , by the ratio of the mass of the astrophysical population,  $M_{astro}$ , to the mass of all the stars in the whole small-scale galaxy in which the fixed population is embedded,  $M_{fixed,stars}$ , as follows:

$$N_{astro} = N_{fixed} \frac{M_{astro,tot}}{M_{fixed,stars}}, \quad (2.1)$$

or by the ratio of the number of stars in the astrophysical population,  $N_{astro,tot}$ , to the total number of stars formed to produce the fixed population,  $N_{fixed,tot}$ ,

$$N_{astro} = N_{fixed} \frac{N_{astro,tot}}{N_{fixed,tot}}. \quad (2.2)$$



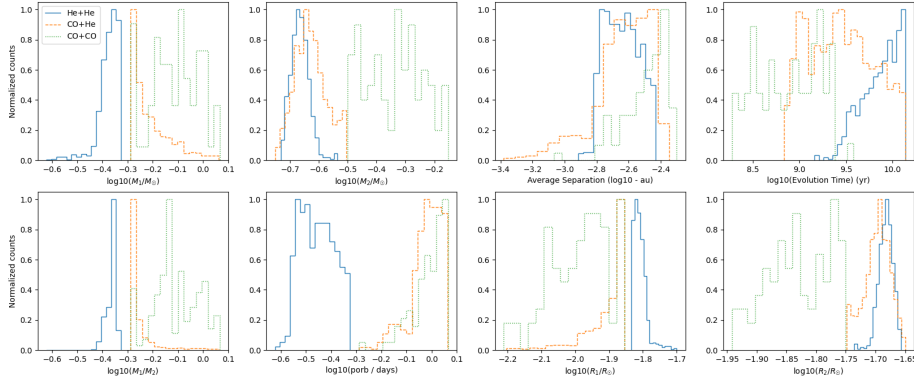


Figure 2.2: Distributions of the parameters of a fixed population with metallicity  $Z = 0.020$  composed of He+He, CO+He and CO+CO binary white dwarfs. This includes the mass, radius of primary and secondary stars, the radius ratios between the two, the orbital period, average separation, and evolution time.

Thus, to create a full-scale astrophysical population we need a *reference population* from which we can extract either the total mass or the total number of stars, to then use to scale up our fixed population. As we will now see, the chosen reference for our purpose is a catalog which reports many key galactic parameters in it, which will allow us to proceed using the method in (2.1).

## 2.3 GWGC and Galaxy Properties

As we have seen, the goal of this work is to simulate the gravitational wave background produced by compact binaries in the *local universe*, by generating the sources using COSMIC. To replicate the existing, observed galaxies in the vicinity of the Milky Way and simulate their stellar content we rely on the dataset provided in White et al. [2011], the **Gravitational Wave Galaxy Catalog (GWGC)**. This catalog includes a list of 53,255 galaxies within  $100Mpc$  from earth, containing information on sky position, distance, blue magnitude, major and minor diameters, position angle, and galaxy type, currently used for follow-up searches of electromagnetic counterparts from gravitational wave searches.

### 2.3.1 What it has vs what we need

In principle, we could generate a separate fixed population for each galaxy in the GWGC and scale it individually. However, this is simply not practical because of the computational power and time it would require, and therefore we must find a strategy to group them in a few, representative, categories. As we will show in this section, many of the information in the GWGC can be used to infer the missing astrophysical quantities we need for population synthesis. Ultimately, we will find

that metallicity is the most suitable parameter for grouping galaxies. To get there, we follow a chain of empirical relations, starting from the galaxy morphological type, through a luminosity to mass, and then a mass to metallicity relation. This process will enable us to provide COSMIC with the necessary input, found in a consistent and astrophysically motivated way.

### 2.3.2 Mass-luminosity relation

As previously discussed, in order to scale a fixed population to the size of a specific galaxy, we need either its total stellar mass or the number of stars. In particular, Faber and Gallagher [1979] presents a luminosity-to-mass relation that depends on the morphological type. This allows to use the blue magnitude and the T-type provided in GWGC to estimate each galaxy's stellar mass.

#### Magnitude to luminosity

To compute the stellar mass, the luminosity-to-mass ratio presented in Faber and Gallagher [1979] applies to the absolute blue luminosity of each galaxy. GWGC provides the absolute blue magnitude, thus we have to convert it into blue luminosity using the Sun's blue-band absolute magnitude as a reference (typically  $M_{B,\odot} = 5.48$ ). Starting from the magnitude definition,

$$m_{B,gal} - m_{B,\odot} = -2.5 \log_{10} \left( \frac{L_{B,gal}}{L_{B,\odot}} \right),$$

which, in stellar units, brings us to the following conversion:

$$L_{B,gal} = 10^{-0.4(m_{B,gal} - m_{B,\odot})} L_{B,\odot} \quad (2.3)$$

where  $m_{B,gal}$  and  $m_{B,\odot} \approx 5.48$  are the absolute blue magnitudes of the specific galaxy and the sun.

#### Galaxy morphological types

Although the GWGC denotes galaxy morphology using the de Vaucouleurs T-type scale, the luminosity-to-mass relations used in Faber and Gallagher [1979] are defined in terms of Hubble morphological classes. This classification is crucial because different morphological types exhibit significantly different stellar populations and star formation histories, which affect both luminosity and mass content. For example, elliptical galaxies generally have lower luminosity-to-mass ratios than spirals due to their older stellar populations and lack of ongoing star formation. Fortunately, a direct correspondence exists between T-type values and Hubble types, and thanks to the results in Faber and Gallagher [1979] we find the following correspondences:

The luminosity resulting from (2.3), expressed in units of solar blue luminosity

T-Value	Hubble Class	$\frac{M}{L_B}$
−6.00 to −4.01	<i>E</i>	8.5
−4.00 to −2.01	<i>S0</i> <sup>−</sup>	9.5
−2.00 to −0.99	<i>S0</i> <sup>+</sup> − <i>S</i> <sub><i>a</i></sub>	6.2
1.00 to 3.99	<i>S</i> <sub><i>ab</i></sub> − <i>S</i> <sub><i>bc</i></sub>	6.5
4.00 to 4.99	<i>S</i> <sub><i>bc</i></sub> − <i>S</i> <sub><i>c</i></sub>	4.7
5.00 to 5.99	<i>S</i> <sub><i>cd</i></sub> − <i>S</i> <sub><i>d</i></sub>	3.9
6.00 to 10.00	<i>S</i> <sub><i>dm</i></sub> − <i>Irr</i>	8.5

Table 2.1: WRITE CAPTION

$L_{B,\odot}$ , can then be multiplied by the appropriate  $M/L_B$  ratio, as in **Table 2.1**, to yield the total stellar mass for the galaxy

$$M_{gal} = \frac{M}{L_B} L_{B,gal} \quad (2.4)$$

### 2.3.3 Mass-metallicity relation

Now that we have estimated the stellar mass of each galaxy, we can also derive the corresponding metallicity. This is made possible by the results of Tremonti et al. [2004], where an empirical relation between stellar mass and gas-phase oxygen abundance (a proxy for galaxy metallicity) is established. The study, based on a sample of over 50,000 star-forming galaxies observed by the Sloan Digital Sky Survey, reveals a tight correlation between stellar mass and metallicity, spanning three orders of magnitude in mass and a factor of ten in metallicity, which can be written as follows:

$$Z' = -1.492 + 1.847 \times \log(M_*) - 0.08026 \times [\log(M_*)]^2, \quad (2.5)$$

where  $M_*$  is the galactic stellar mass, and

$$Z' = 12 + \log(O/H) \quad (2.6)$$

is the metallicity written in terms of the oxygen abundance (all the metallicity values with an apostrophe are intended as in these units).

#### On metallicity units

Now, in these units the sun's metallicity is<sup>3</sup>  $Z'_\odot = 8.69$ , whereas in the units used by COSMIC it is<sup>4</sup>  $Z_\odot = 0.0134$  (all the metallicity values without the apostrophe are intended as in these units). We can easily find a conversion between the two unit

<sup>3</sup>This value is taken from the work Allende Prieto et al. [2001]

<sup>4</sup>This refers to the work Asplund et al. [2009]

systems by assuming that the rate of oxygen abundance in the galaxy and the one in the sun is equal to the rate of the metallicities in COSMIC's units,

$$\frac{(O/H)_{gal}}{(O/H)_{\odot}} = \frac{Z_{gal}}{Z_{\odot}}, \quad (2.7)$$

where  $(O/H)$  can be found inverting (2.6). At this point, knowing that  $Z'_{\odot} = 8.69$ , we can:

- Compute the  $Z'_{gal}$  value for each galaxy in GWGC using (2.5);
- Write  $(O/H)_{\odot}$  and  $(O/H)_{gal}$  in terms of the corresponding  $Z'$  value using (2.6):  $(O/H) = 10^{(Z'-12)}$  and  $(O/H)_{\odot} \approx 0.32$ .

Finally, finding  $Z_{gal}$  from (2.7), we can write the metallicity units conversion as:

$$Z_{gal} = 27.3 \times 10^{(Z'-12)}, \quad (2.8)$$

where the "27.3" coefficient mainly depends on the  $Z_{\odot}$  value. This relation allows us to assign a realistic metallicity estimate to each GWGC galaxy in COSMIC's units, which we can now use to group them into representative subsets. This way, we can account for the significant impact of metallicity on stellar wind strength, remnant masses, and binary evolution outcomes, that greatly affects the expected gravitational wave signal.

### 2.3.4 Missing galaxies

The GWGC is far from being a complete list of the galaxies in the local Universe. As we will now see, there are two main factors contributing to this incompleteness: observational limitations due to the Zone of Avoidance (ZOA) and limitations of the information that the catalog presents.

#### Zone of avoidance

Since the GWGC is an observation-based catalog compiled from optical surveys, we must account for the Zone of Avoidance — the region of the sky obscured by the Milky Way's interstellar dust and stellar crowding, which impedes the detection of background galaxies. The extent of the ZOA depends on the wavelength of observation: infrared surveys penetrate deeper through the dust, while optical surveys, like those used for GWGC, are more strongly affected. In the optical band, the ZOA is expected to cover about  $\sim 25\%$  of the sky Kraan-Korteweg and Lahav [2000]. For this work, we estimated the ZOA directly from the spatial distribution of galaxies in GWGC, by plotting their positions in Galactic coordinates. This way, the ZOA appears clearly as a horizontal band centered around the Galactic plane (see **Figure 2.3**). To quantify its extent, we divided the sky map into  $n_{\text{pix}}$  equal-area pixels and focused on the band  $|b| \leq 15^\circ$  in Galactic latitude. Counting the empty pixels

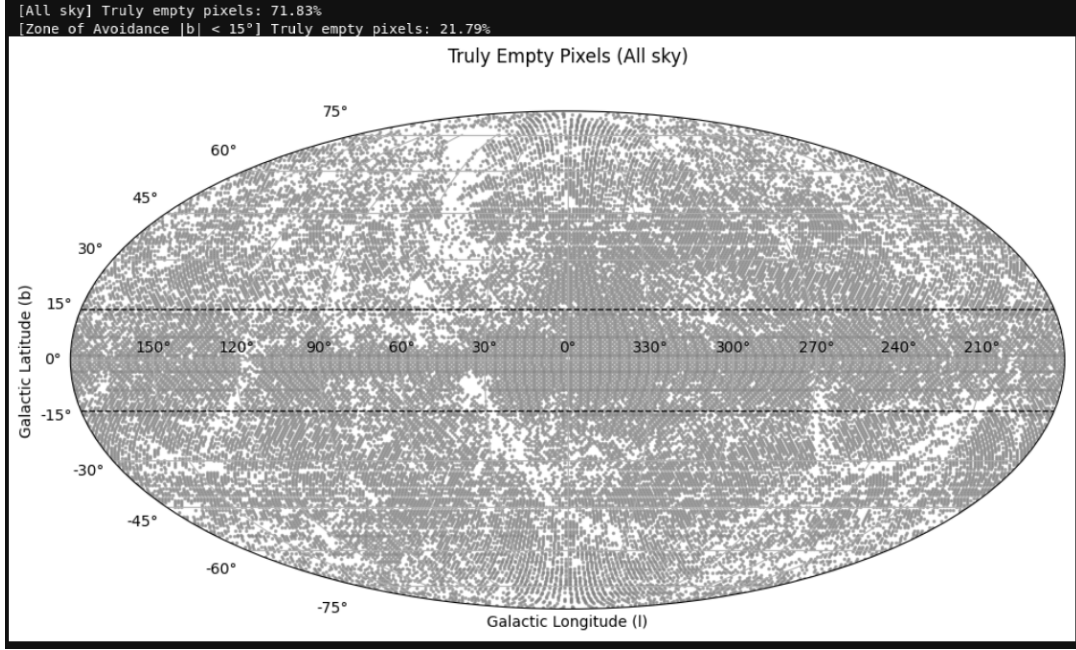


Figure 2.3: INSERT CAPTION AND REDO IMAGE IN PDF!!!

in this band and dividing by  $n_{\text{pix}}$  gives an estimated ZOA coverage of  $\sim 20\%$ – $25\%$  of the sky, depending on the chosen pixel resolution. This estimate is fully consistent with the literature Kraan-Korteweg and Lahav [2000], so in our analysis we will assume that GWGC effectively covers  $\sim 80\%$  of the sky.

### Incompleteness and non-galactic objects

Secondly, the entries of the GWGC represent a source of incompleteness themselves. Not all the objects listed in the GWGC are suitable for our purposes: in addition to galaxies, the catalog also includes globular clusters, which can be identified through their T-type values; moreover, not all galaxies in the catalog contain all the information required to perform the procedures described in the previous sections. To construct a working sample, we applied a series of masks to clean the catalog:

- Only keep entries classified as galaxies;
- Require that the distance, T-type, and absolute blue magnitude are provided;

After this selection, the sample we are left with reduced from the original 53,255 entries to roughly 20,000 galaxies suitable for population synthesis.

### Filling the gap

In order to compensate the missing galaxies, we have make two physically motivated assumptions.

### 1. Cosmological Principle:

The GWGC lists all the observed galaxies within  $100\text{Mpc}$ . On such scales, the Universe can be assumed to be statistically *homogeneous* and *isotropic*. This assumption is supported from observations of the *Cosmic Microwave Background* (CMB), where we know that the correlation function of the temperature fluctuations across the sky peaks at scales of  $\sim 100\text{Mpc}$ . Under this assumption, the selected galaxies of the GWGC should be statistically representative of the overall population in the same volume.

### 2. Distance Matters:

The angular position is irrelevant in the computation of the gravitational wave signal; only the distance of the source matters. Therefore, missing galaxies from the unexplored volume covered by the Milky Way can be statistically represented by the galaxies from our retained sample.

Following these assumptions, we “fill in” the missing fraction of the sky and the dropped entries of the catalog by sampling with replacement from the cleaned GWGC, just like we did to extract an astrophysical from the fixed one, preserving its parameter distributions. This ensures that the statistical properties of the synthetic galaxy distribution match those of the observed portion while restoring the full-sky coverage. This is shown in a graphical representation of the distributions of distances, blue band magnitudes and T-types, in **Figure 2.4**: the distributions have been scaled up without visible changes.

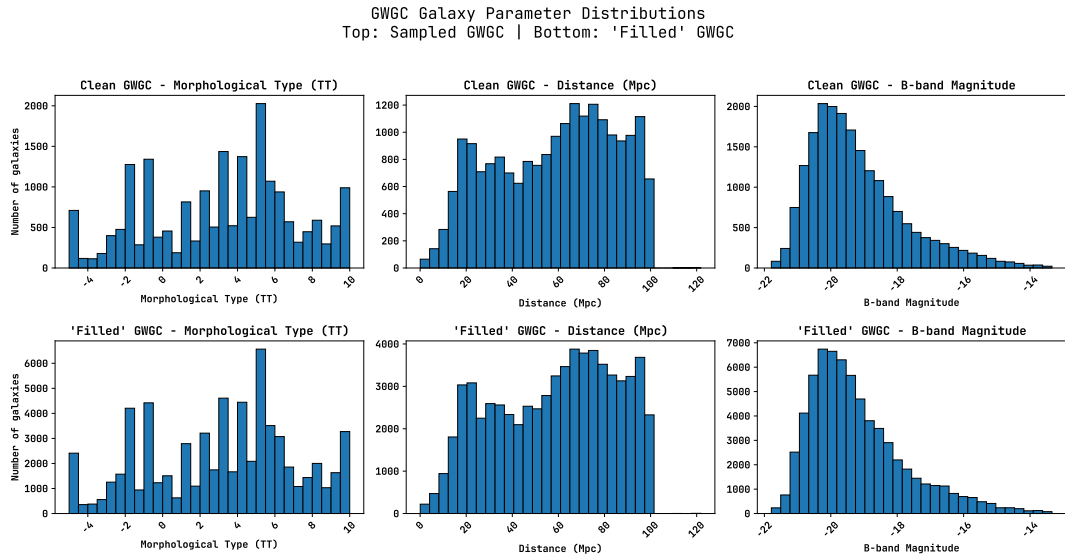


Figure 2.4: INSERT CAPTION

## 2.4 Final considerations

Now that the catalog has been completed and its ready for the population synthesis, its time to put all the pieces together. What we will do in this last section, is to generate the fixed populations that will represent all the galaxies in the final catalog, scale them accordingly, compute the gravitational wave signal of all the binaries they contain, and finally compare it with LISA's sensitivity curve.

### 2.4.1 The final fixed populations

As we already discussed, the metallicity of a galaxy has a great impact on the stellar evolution and, thus, gravitational wave signal. This, plus the fact that metallicity is closely linked to the galaxy types too, led us to choose it as characterizing parameter for the populations that we will generate to represent the galaxy in the catalog. In particular, we the final catalog covers a range from a minimum of  $Z = 0.00748$  to a maximum of  $Z = 0.03948$ . We decided to group all the values in between in ten equally wide bins, represented in **Figure 2.5**.

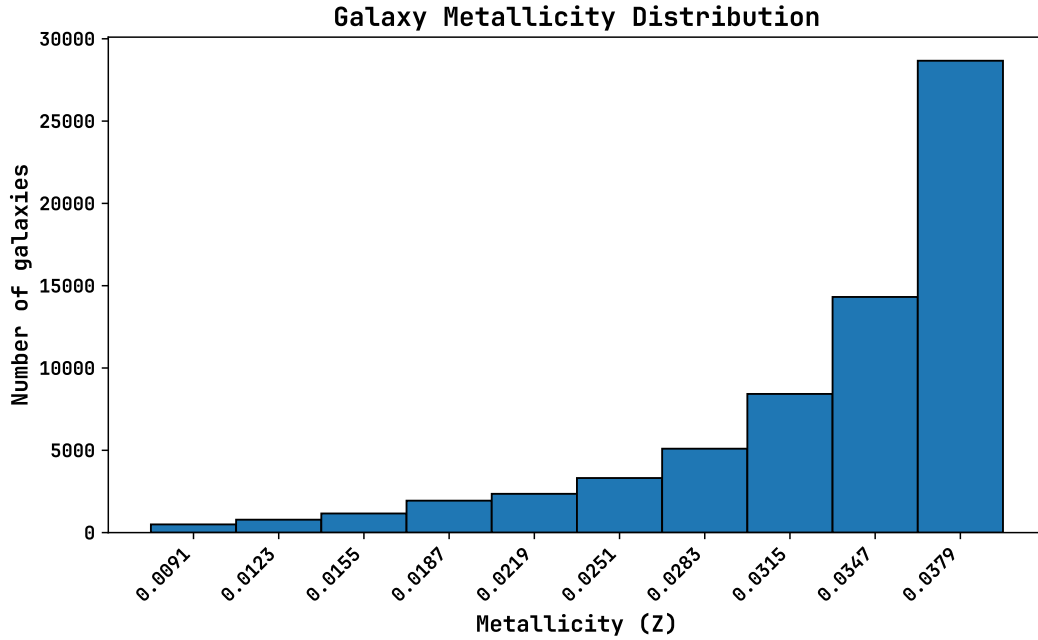


Figure 2.5: insert caption

Each one of the center values of the bins, shown in the  $x$  label, is linked to a different synthetic fixed population generated with COSMIC. For this thesis project, the fixed populations we generated covered the  $k$ star values 10, 11 and 12, corresponding to He, CO, and Ne white dwarfs<sup>5</sup>. The simulation was done using ASK WILL INFO ON COSMIC-POP COMMAND USED.

<sup>5</sup>INSERISCI TABELLA IN APPENDICE, E QUI IL RIERIMENTO

### 2.4.2 LISA's frequency resolution

#### Sum gw signal

ASD and multiple sources signal addition

#### LISA frequency bins

LISA  $T_{obs}$

#### The signal computation IN RESULTS?

At this point we are fully equipped to be able to compute the gravitational wave signal of the sources. This will be done in an iterative process applied to each galaxy in the final catalog, which consists of the following steps:

- Compute the right  $N_{astro}$  using the (2.1)
- Scale the fixed population accordingly, thus creating the full-scale galaxy simulation. At this point for each binary system in this astrophysical population we:
  - Compute each binary's gravitational wave signal using (??);
  - Bin this signal to LISA's frequency bins, by summing it using (??);
  - Plot this value on LISA's curve.



# Chapter 3

## Results

- Plot of spectral distribution of the computed signal - Analysis of the distribution of the sources - Eventual implications (none, since it shouldn't be visible)



## Chapter 4

# Conclusions and Future Perspectives

Recap of the whole Work - Limits of the Work, assumptions and approximations used - Possible extensions



# Appendix A

## Appendix

Dettagli tecnici sul codice.

Tabelle di parametri.

Ulteriori grafici.

Script di calcolo, se rilevante.

INSERISCI TABELLE COI KSTAR VALUES ETC



# Bibliography

- Carlos Allende Prieto, David L. Lambert, and Martin Asplund. The Forbidden Abundance of Oxygen in the Sun. *ApJ*, 556(1):L63–L66, July 2001. doi: 10.1086/322874.
- Martin Asplund, Nicolas Grevesse, A. Jacques Sauval, and Pat Scott. The Chemical Composition of the Sun. *ARA&A*, 47(1):481–522, September 2009. doi: 10.1146/annurev.astro.46.060407.145222.
- Katelyn Breivik, Scott Coughlin, Michael Zevin, Carl L. Rodriguez, Kyle Kremer, Claire S. Ye, Jeff J. Andrews, Michael Kurkowski, Matthew C. Digman, Shane L. Larson, and Frederic A. Rasio. COSMIC Variance in Binary Population Synthesis. *ApJ*, 898(1):71, July 2020. doi: 10.3847/1538-4357/ab9d85.
- Katerina Chatziioannou, James Alexander Clark, Andreas Bauswein, Margaret Millhouse, Tyson B. Littenberg, and Neil Cornish. Inferring the post-merger gravitational wave emission from binary neutron star coalescences. *Phys. Rev. D*, 96(12):124035, December 2017. doi: 10.1103/PhysRevD.96.124035.
- S. E. de Mink, O. R. Pols, and R. W. Hilditch. Efficiency of mass transfer in massive close binaries. Tests from double-lined eclipsing binaries in the SMC. *A&A*, 467(3):1181–1196, June 2007. doi: 10.1051/0004-6361:20067007.
- Michal Dominik, Krzysztof Belczynski, Christopher Fryer, Daniel E. Holz, Emanuele Berti, Tomasz Bulik, Ilya Mandel, and Richard O’Shaughnessy. Double Compact Objects. I. The Significance of the Common Envelope on Merger Rates. *ApJ*, 759(1):52, November 2012. doi: 10.1088/0004-637X/759/1/52.
- S. M. Faber and J. S. Gallagher. Masses and mass-to-light ratios of galaxies. *ARA&A*, 17:135–187, January 1979. doi: 10.1146/annurev.aa.17.090179.001031.
- Aaron M. Geller, Nathan W. C. Leigh, Mirek Giersz, Kyle Kremer, and Frederic A. Rasio. In Search of the Thermal Eccentricity Distribution. *ApJ*, 872(2):165, February 2019. doi: 10.3847/1538-4357/ab0214.
- D. Goldberg and T. Mazeh. The mass-ratio distribution of the spectroscopic binaries in the Pleiades. *A&A*, 282:801–803, February 1994.

- D. C. Heggie. Binary evolution in stellar dynamics. *MNRAS*, 173:729–787, December 1975. doi: 10.1093/mnras/173.3.729.
- Jarrold R. Hurley, Onno R. Pols, and Christopher A. Tout. Comprehensive analytic formulae for stellar evolution as a function of mass and metallicity. *MNRAS*, 315(3):543–569, July 2000. doi: 10.1046/j.1365-8711.2000.03426.x.
- Jarrold R. Hurley, Christopher A. Tout, and Onno R. Pols. Evolution of binary stars and the effect of tides on binary populations. *MNRAS*, 329(4):897–928, February 2002. doi: 10.1046/j.1365-8711.2002.05038.x.
- J. Klencki, M. Moe, W. Gladysz, M. Chruslinska, D. E. Holz, and K. Belczynski. Impact of inter-correlated initial binary parameters on double black hole and neutron star mergers. *A&A*, 619:A77, November 2018. doi: 10.1051/0004-6361/201833025.
- Renée C. Kraan-Korteweg and Ofer Lahav. The Universe behind the Milky Way. *A&A Rev.*, 10(3):211–261, January 2000. doi: 10.1007/s001590000011.
- Pavel Kroupa. On the variation of the initial mass function. *MNRAS*, 322(2):231–246, April 2001. doi: 10.1046/j.1365-8711.2001.04022.x.
- Pavel Kroupa, Christopher A. Tout, and Gerard Gilmore. The Distribution of Low-Mass Stars in the Galactic Disc. *MNRAS*, 262:545–587, June 1993. doi: 10.1093/mnras/262.3.545.
- Tsevi Mazeh, Dorit Goldberg, Antoine Duquennoy, and Michel Mayor. On the Mass-Ratio Distribution of Spectroscopic Binaries with Solar-Type Primaries. *ApJ*, 401:265, December 1992. doi: 10.1086/172058.
- Maxwell Moe and Rosanne Di Stefano. Mind Your Ps and Qs: The Interrelation between Period (P) and Mass-ratio (Q) Distributions of Binary Stars. *ApJS*, 230(2):15, June 2017. doi: 10.3847/1538-4365/aa6fb6.
- Edwin E. Salpeter. The Luminosity Function and Stellar Evolution. *ApJ*, 121:161, January 1955. doi: 10.1086/145971.
- Christy A. Tremonti, Timothy M. Heckman, Guinevere Kauffmann, Jarle Brinchmann, Stéphane Charlot, Simon D. M. White, Mark Seibert, Eric W. Peng, David J. Schlegel, Alan Uomoto, Masataka Fukugita, and Jon Brinkmann. The Origin of the Mass-Metallicity Relation: Insights from 53,000 Star-forming Galaxies in the Sloan Digital Sky Survey. *ApJ*, 613(2):898–913, October 2004. doi: 10.1086/423264.
- L. M. van Haaften, G. Nelemans, R. Voss, S. Toonen, S. F. Portegies Zwart, L. R. Yungelson, and M. V. van der Sluys. Population synthesis of ultracompact X-ray binaries in the Galactic bulge. *A&A*, 552:A69, April 2013. doi: 10.1051/0004-6361/201220552.



---

Darren J White, E J Daw, and V S Dhillon. A list of galaxies for gravitational wave searches. *Classical and Quantum Gravity*, 28(8):085016, March 2011. ISSN 1361-6382. doi: 10.1088/0264-9381/28/8/085016. URL <http://dx.doi.org/10.1088/0264-9381/28/8/085016>.